Progress In Electromagnetics Research C, Vol. 126, 91–103, 2022

Low Profile Textile Flower-Shaped Antenna for Ultra Wideband Applications

Samanthapudi Bhavani* and Thangavelu Shanmuganantham

Abstract—In this paper, a miniaturized Ultra-Wideband (UWB) flower-shaped radiator antenna is designed and simulated for 2.9 GHz to 14.8 GHz applications in Wireless Body Area Networks (WBAN). To achieve wideband, two alterations have been incorporated into the proposed design, i.e., by adopting a flower-shaped patch to enhance bandwidth and by using the defective ground plane, which reduces capacitive effects, increasing impedance matching within the operating band. This innovative antenna has a footprint of 15 mm × 20 mm × 1.6 mm and uses textile material denim as its substrate, making it compatible with portable UWB devices. Aside from these characteristics, the device also has omnidirectional radiation patterns, a peak gain up to 5 dB, and a fidelity factor over 85%. It is found that the simulation and measurement results are in good agreement. In comparison with existing structures, the antennas obtained show wide operating ranges and compact dimensions.

1. INTRODUCTION

Ultra-wideband (UWB) technology is a very appealing and promising breakthrough in today's wireless communication networks because of its large bandwidth and data rate. Since the Federal Communications Commission (FCC) approved the use of 3.1–10.6 GHz for unlicensed purposes in 2002 [1], UWB technology has grown stronger. By adjusting several factors like data rate, range, power, and quality of service, UWB technology offers a great deal of flexibility for optimizing system performance. Multiple applications can use wireless communication services provided by a single system without the need for extra hardware. Low power and high data rate can be accomplished for short-distance applications, for instance. Under a noise floor where the quality of communication is also preserved, the UWB signals are sent at low power levels. For the other wireless operational signals, these signals are essentially invisible. As a result, there will be no interference issues with other services. The UWB systems benefit from a longer battery life thanks to this low-power function. Communications are secure and dependable thanks to UWB technology. UWB signals are extremely difficult to detect since they are used at low powers below the noise level. The noise interferes with the UWB signals notwithstanding their ability to be retrieved. As a result, UWB signals are particularly effective in facilitating dependable and secure connections. There is no need to modulate or demodulate the UWB signals (no up conversion and down conversion). As a result, modules like mixers, extra oscillators, amplifiers, filters, etc. are not needed for UWB systems. This benefit aids in lowering the price, level of complexity, and size of devices. Furthermore, employing these brief, narrow pulses, several modulation techniques, including pulse amplitude modulation (PAM), pulse position modulation (PPM), and phase shift keying, can be applied.

Planar antennas are suitable for portable devices in wireless communication systems. They employ several antenna structures to attain UWB performance [2–27]. For the use in UWB applications, a unique U-shaped microstrip-patch antenna [2] with dimensions of 24 mm × 28 mm × 0.787 mm is

Received 22 September 2022, Accepted 27 October 2022, Scheduled 3 November 2022
* Corresponding author: Samanthapudi Bhavani (ammav10@gmail.com).
The authors are with the Pondicherry University, India.

suggested. Its bandwidth spans the range of 2.76 GHz to 12.8 GHz, and its highest peak gain is 5.3 dBi at 10.2 GHz. It is suggested to use a tiny UWB microstrip antenna that is fed by a coplanar waveguide (CPW) and measures 25 mm × 25 mm × 1.6 mm [3]. Its bandwidth spans the frequency range of 2.6 GHz to 13.04 GHz, and its highest peak gain is 4.25 dBi at 11.78 GHz.

[4] proposed a novel structure with dimensions of 40 mm × 48 mm × 1.6 mm and an operating frequency band of 3.06 to 12.37 GHz. Graphene is used as a substrate in antenna design [12], which operates at 3.5 & 5.8 GHz. In [13], the authors present a UWB planar antenna with defected ground structure (DGS) for various wireless applications.

A novel shape of a hexagonal slot in a rectangular step shape patch with a partial ground plane is developed with a bandwidth of 12 GHz in [14]. The design and analysis of a V-shaped UWB antenna and dual-band UWB notch antenna with dimensions of $28 \times 23\,\text{mm}^2$ are proposed in [15]. Wearable UWB antennas are also designed for medical applications [19–27].

In this work, we present a UWB antenna that is small and has an exceedingly straightforward construction. The radiating element comprises five elliptically shaped patches that are 20 degrees apart and resemble flowers. To widen the frequency range through resonance, the branches of the modified ground structure are employed on the one hand to generate various frequencies.

The format of this work is as follows. Section 2 covers the design of a flower-shaped antenna (from initial step on words), analysis of ground parameters, and current distribution. Simulation results are included in Section 3. Section 4 provides specifics of the conclusions.

2. FLOWER-SHAPED ANTENNA DESIGN

2.1. Antenna Geometry

The proposed flower-shaped UWB antenna system is shown in Fig. 1 along with its architecture. The antenna system suggested in this study has a small size of $20 \times 15\,\text{mm}^2$, and it was created on a substrate made of denim with 1.6 mm thickness ($r = 1.7$) and copper material as ground and patch. This antenna system is smaller than those published in the literature. The overall antenna concept consists of a metal ground, a radiating element in the form of a flower, and other components. Five elliptically shaped patches are positioned above the substrate, each at a 20-degree angle from the others, and together they form the radiating element that resembles a flower and is directly fed by a microstrip line. Next,

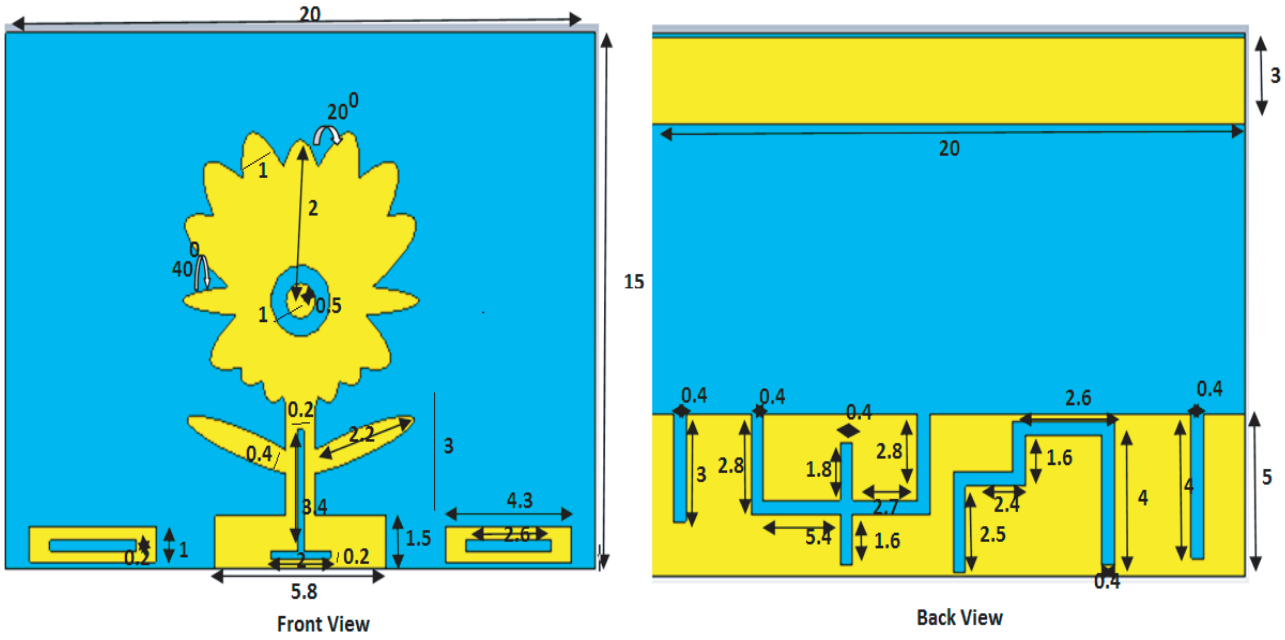

Figure 1. Contour of the proposed flower-shaped antenna.

Table 1. Parameters of the flower-shaped antenna.

Parameter	Dimensions
Substrate	$15 \times 20 \times 1.6\,\text{mm}^3$
Operating range	2.9–14.8 GHz
Peak Gain	4.9 dBi at 5.2 GHz
Polarization	Linear

mirror-symmetric rectangular patches with slots and enhanced, leaf-shaped branches are implemented. Additionally, the feed slot is inverted T-shaped. To achieve a reflection coefficient below −10 dB for a wide range of frequencies, the ground plane has been redesigned by combining various slots with a partial ground structure. Table 1 displays the antenna's dimensions and performance parameters. This compact UWB antenna prototype is printed on a denim substrate to justify and validate the simulation results. Fig. 2(a) shows the prototype of the proposed antenna design. An experimental test of this antenna model was conducted using an Agilent N5247A analyzer in the frequency range of 0 to 20 GHz, as shown in Fig. 2(b) for ensuring UWB capability with a very attractive $20 \times 12\,\text{mm}^2$ size.

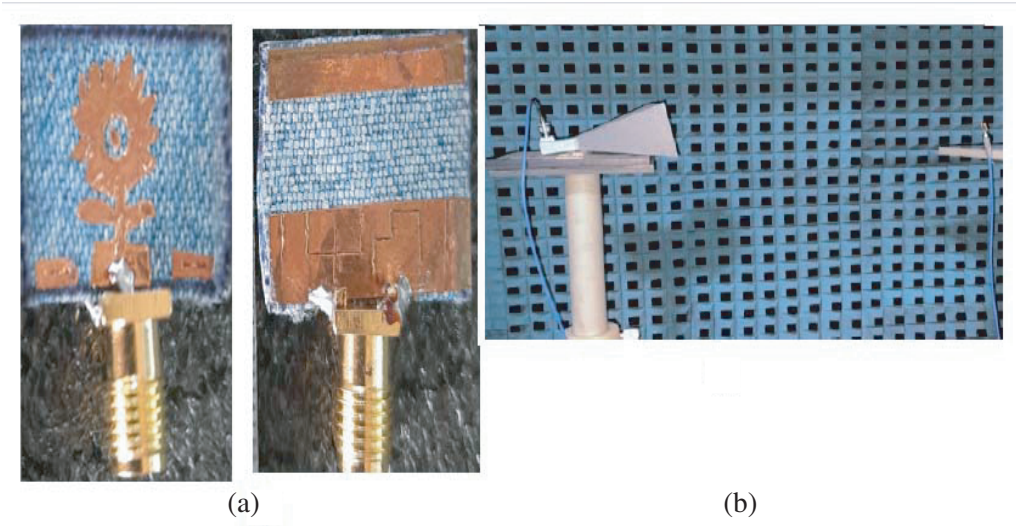

Figure 2. Testing: (a) prototype, (b) anechoic chamber view.

2.2. Evaluation of Flower-Shaped Antenna

The 50 ohm transmission line feed and fractional ground plane are combined to study the effects of various antenna layouts. Figs. 3 and 4 describe the proposed UWB antenna system's operating principle utilizing reflection coefficient curves, respectively, while Fig. 3 elaborates on the whole design process.

In its first stages, the radiating element consists of five elliptical patches that are perpendicular to one another, a microstrip line, and a full rectangular ground at the bottom. The antenna, which was initially constructed with five elliptical patches, has a poor reflection coefficient and the best value for S_{11} of just −24.18 dB, as shown in Fig. 4. As a result, in stage 1, the radiating element is changed to resemble a flower by combining five elliptically shaped patches, while the ground structure is left unaltered.

The impedance-matching performance of this antenna configuration is enhanced, and it produces a resonant mode at 6.10 GHz with a reflection coefficient of −28.2 dB. In stage 2, a new rectangular patch is added to the top of the ground, improving impedance matching and lowering the S_{11} value to −42.8 dB. In stage 3, the number of slots is increased as depicted in the figure. This produces three

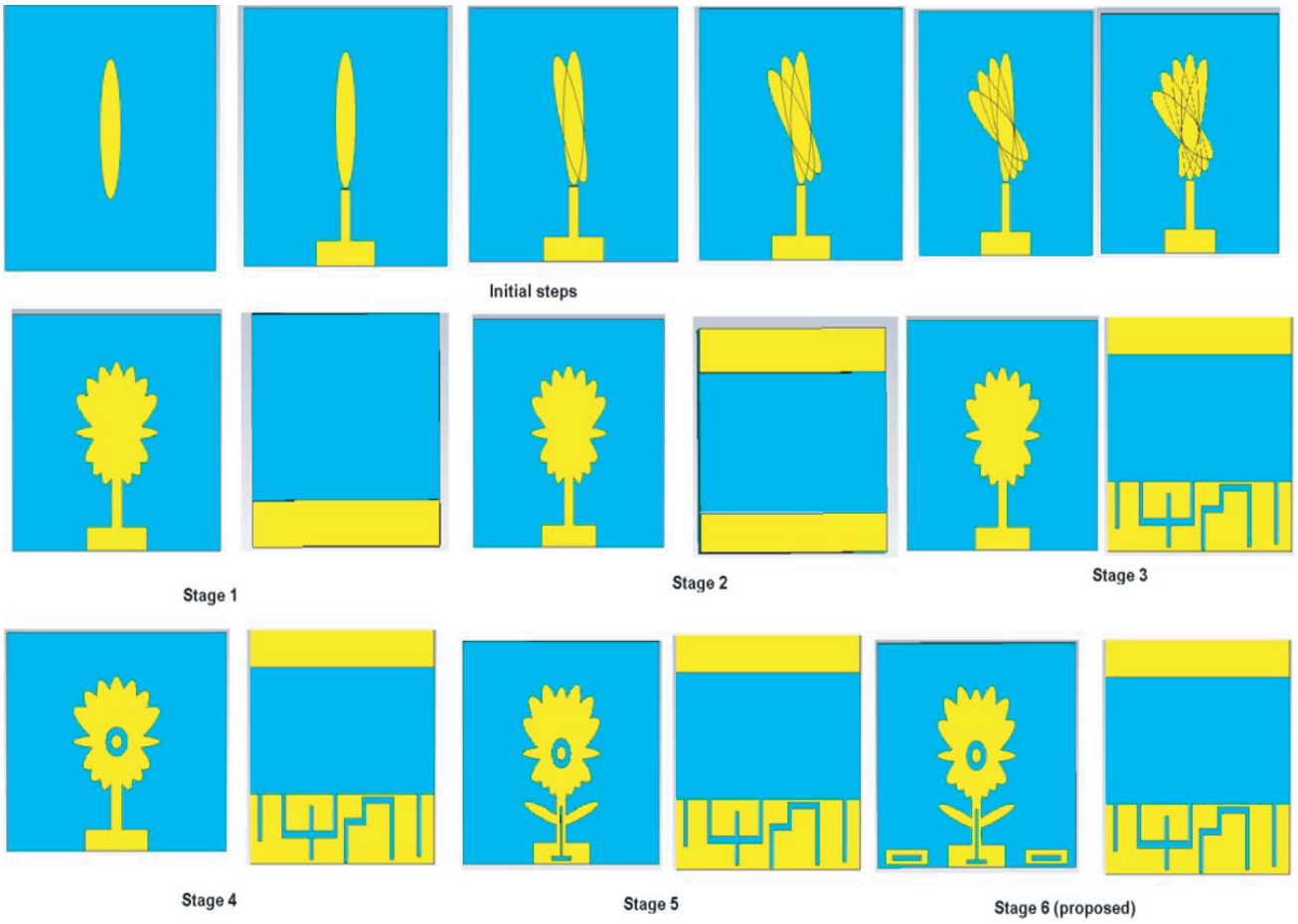

Figure 3. Evaluation of the flower-shaped design.

resonant frequencies, with S_{11} having the best value at −58.7 dB. To increase the impedance bandwidth, a circular hole with an inner radius of 0.5 mm and outer radius of 1 mm is added to the flower in stage 4. In stage 5, an inverted T-shaped slot is added to the feed to increase bandwidth, and S_{11} is −63.29 dB. As of stage 6, the suggested antenna's operational frequency range is enhanced to 2.9–14.8 GHz with the best S_{11} of −71.9 dB.

2.3. Parametric Analysis

In this section, various parametric studies performed on the proposed antenna are reported. The effect of top and bottom rectangular patches on the ground on the reflection coefficient is mainly observed. The performance of the UWB antenna's impedance-matching depends on the lengths of the rectangular ground patches at the top and bottom, which are L_g and L_f, respectively. The only aspect that is studied is how these specific characteristics affect system performance; all other variables are held constant. Fig. 5 shows the S-parameters for tuning L_g from 3 mm to 6 mm. When L_g increases from 3 mm to 6 mm, the impedance bandwidth is significantly enhanced, as seen in the figure. When L_g is 3 mm, 6 mm, or 4 mm, neither UWB feature can be realized.

These findings show that the length of the L_g has a substantial impact on the system's S-parameters, and it is recommended that L_g be set at a value of 5 mm to account for the system's size. Fig. 6 shows the simulated variation in L_f from 2 mm to 4 mm, and at 3 mm the return loss is enhanced.

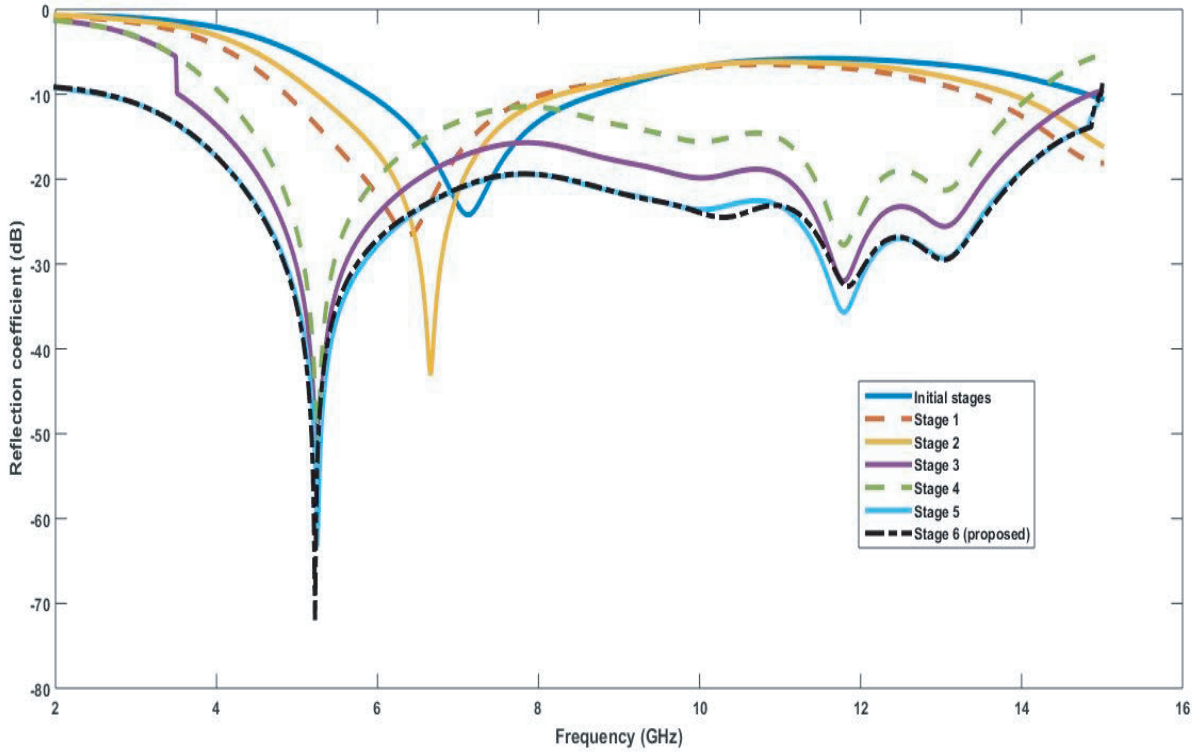

Figure 4. Reflection coefficients comparison for all stages.

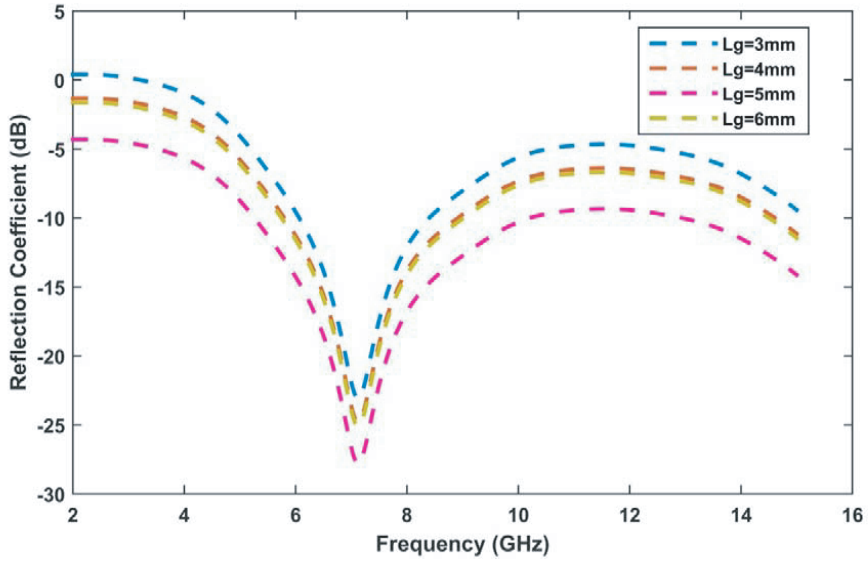

Figure 5. S_{11} performance for variation in L_g.

2.4. Surface Current Distribution in Proposed Antenna

Figure 7 presents the surface current distribution of the antenna at 5.2 GHz, 10.1 GHz, 11.7 GHz, and 13 GHz. From the figure, it can be inferred that strong surface currents reside in the ground plane at higher frequencies. This is because as mentioned earlier the ground rectangular slots are responsible

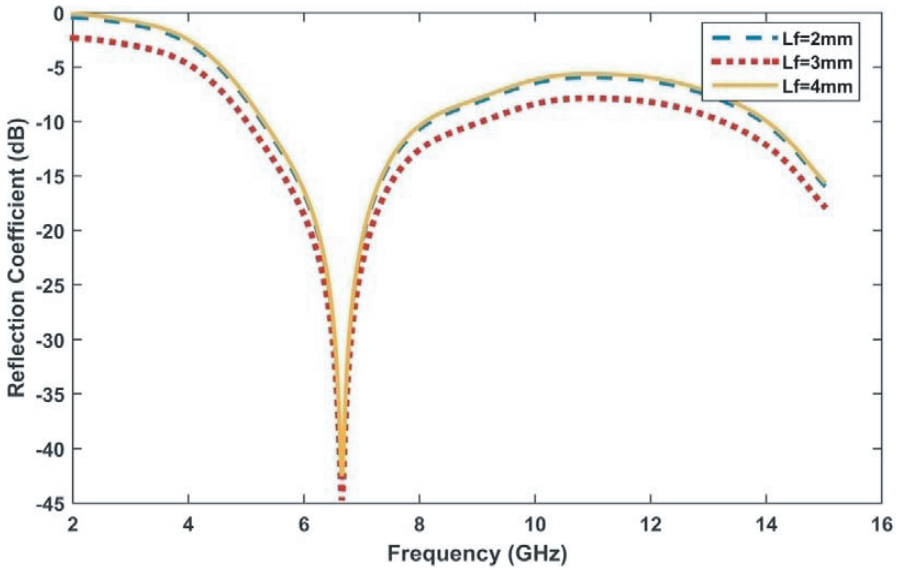

Figure 6. S_{11} performance for variation in L_f.

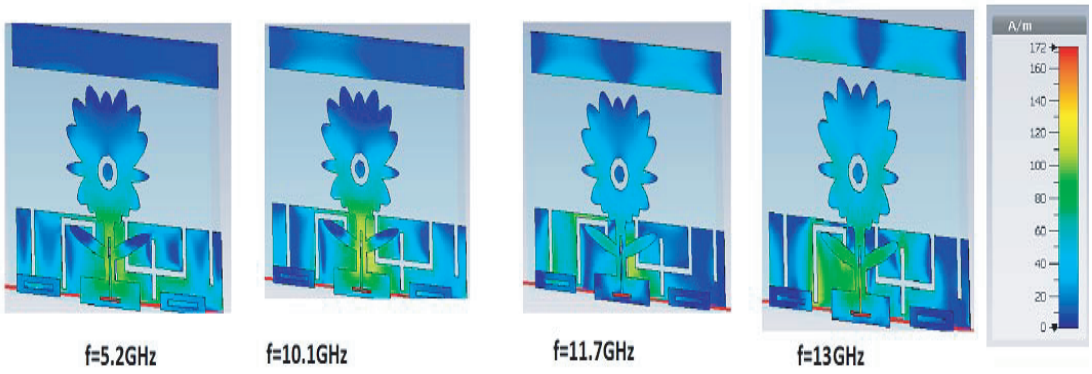

Figure 7. Surface current distribution of flower shaped antenna.

for producing resonating frequencies at the higher operating band. From this observation, it can also be confirmed that the different slots on the ground plane produce a band at higher frequencies.

3. RESULTS AND DISCUSSION

3.1. S-Parameter Results

The results of simulating and measuring the suggested antenna with CST and an Agilent N5247A vector network analyzer are shown in Fig. 8. The observed S_{11} has a range of 3.51–13.8 GHz with a maximum value of −60.2 dB. It is important to remember that there are sizable discrepancies between the measured and simulated outcomes because of manufacturing and measurement mistakes, but these disparities do not have an impact on the system's overall performance. These results support the idea that the suggested antenna provides strong isolation and a wide operating spectrum. Fig. 9 displays that peak realized gain has a value between 0.5 and 4.9 dB in the operating frequency range. Fig. 10 shows the intended antenna's input impedance, which consists of a real part, Re(Z) of nearly 50 Ω, and an imaginary part, Im(Z) of extremely small impedance, for a total input impedance of 50 across its operational spectrum. Mismatch losses are decreased since the input impedance of the antenna and the characteristic impedance of the connector are equivalent.

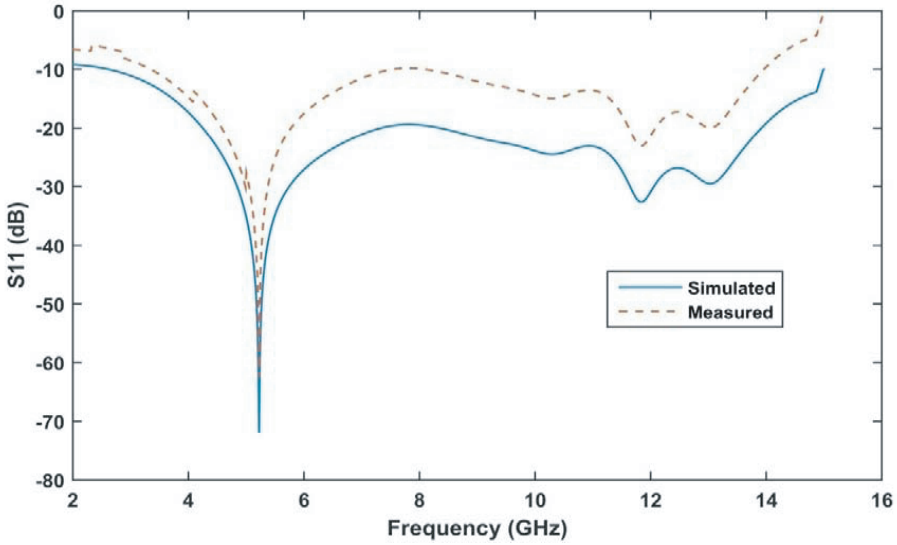

Figure 8. Simulated S_{11} vs measured S_{11}.

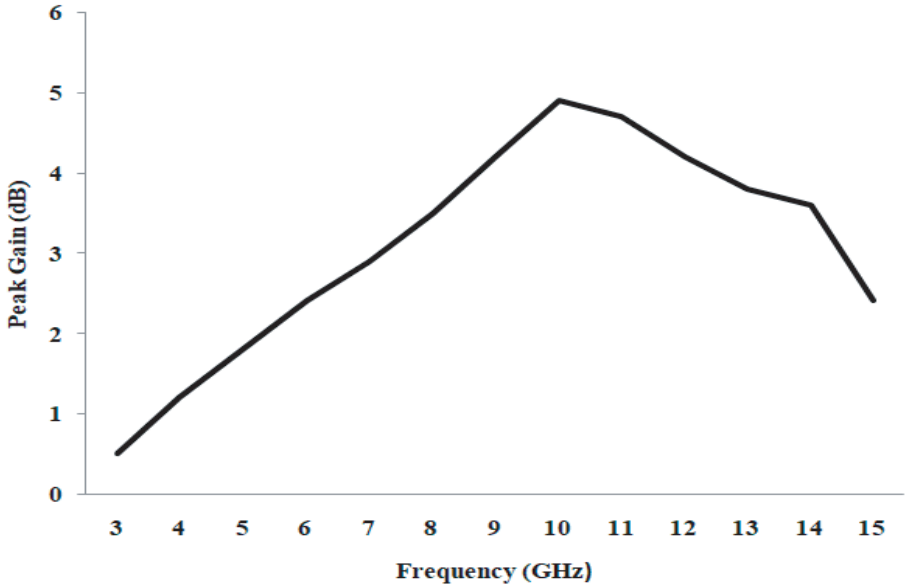

Figure 9. Simulated gain vs frequency.

3.2. Far-Field Properties

Figure 11 shows the results of the UWB antenna test conducted in an anechoic room. The chamber's working frequency ranges from 700 MHz to 18 GHz with dimensions of 5.7 m × 3.5 m × 3 m. Figures 9(a), (b), & (c) show that the antenna almost achieved omnidirectional operation in the two planes at low frequencies. The relevant radiation patterns were recorded by stimulating the port. The XOZ surface almost achieved omnidirectionality at 11.7 GHz. This is mostly caused by the antenna structure and wavelength reduction with frequency.

Figure 12 shows that the difference between the co-polarization and cross-polarization patterns is inversely proportional to frequency in both planes, i.e., the E- and H-planes. The difference is getting smaller, going from 20 to 0 dB. Bidirectional and omnidirectional co-polarization patterns are seen at 5.2 GHz in the E and H planes, respectively. Higher modes may be stimulated at the remaining

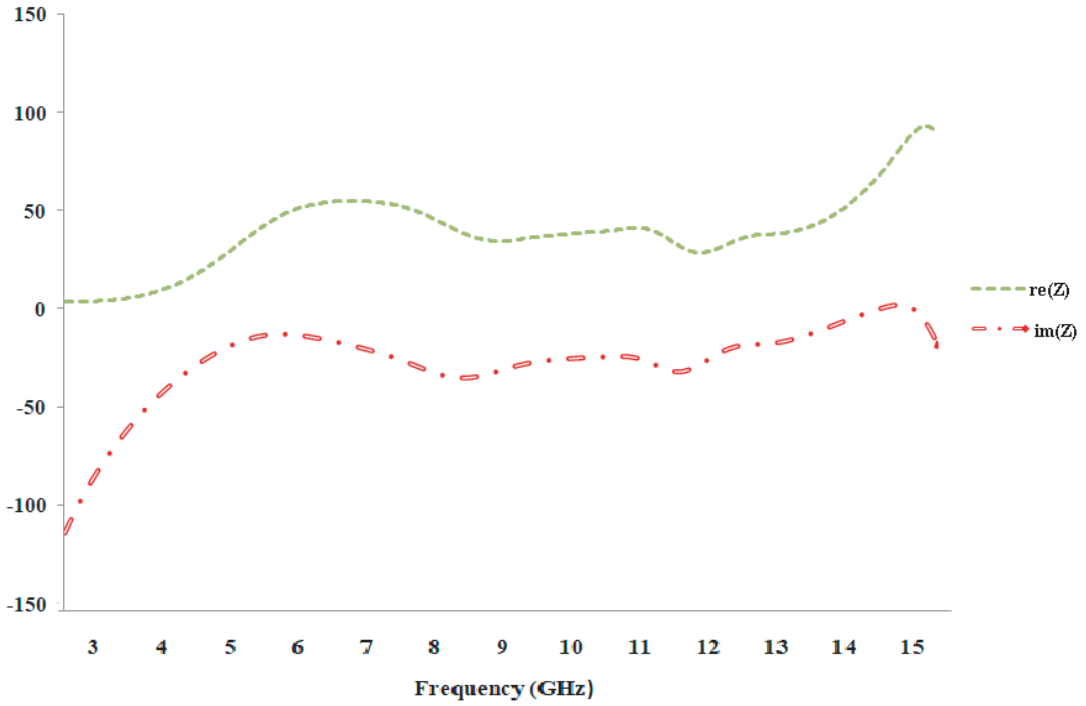

Figure 10. Input impedance characteristics of designed antenna.

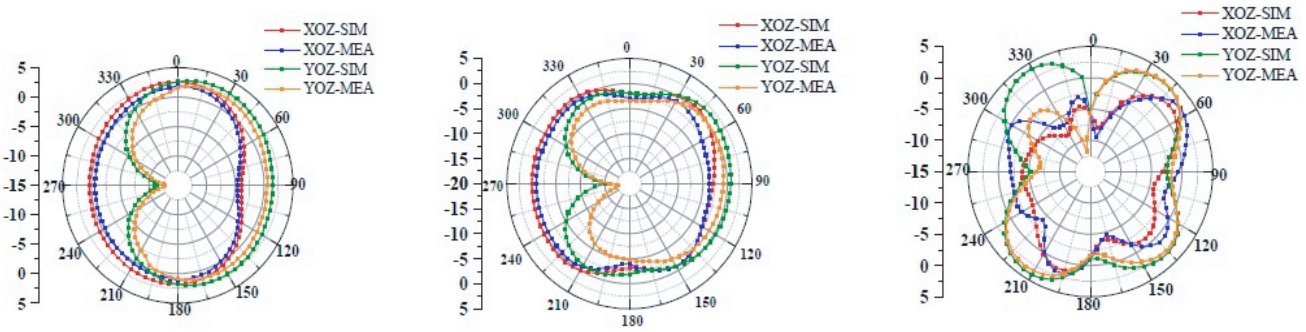

Figure 11. Far-field patterns on XOZ and YOZ planes at (a) 5.2 GHz, (b) 10.1 GHz & (c) 11.75 GHz.

Table 2. Flower-shaped antenna simulated vs measured parameters.

Parameter	Simulation	Measurement
S_{11} Range	2.9–14.8 GHz	3.8–6.5 GHz & 8–13.8 GHz
Impedance Bandwidth	11.9 GHz	2.7 & 5.8 = 8.5 GHz
Max. Peak Gain (dBi)	4.10 dBi at 5.2 GHz	3.9 dBi at 5.2 GHz
Radiation efficiency	88.55%	87.50%

resonances of 10.1 and 11.75 GHz, giving all patterns a twisted omnidirectional form.

Table 2 provides a comparison chart of measured and simulated performances. Table 2 suggests that there is good agreement between the simulated and measured outcomes. The proposed UWB antenna is compared to existing conventional-type antenna configurations documented in the literature

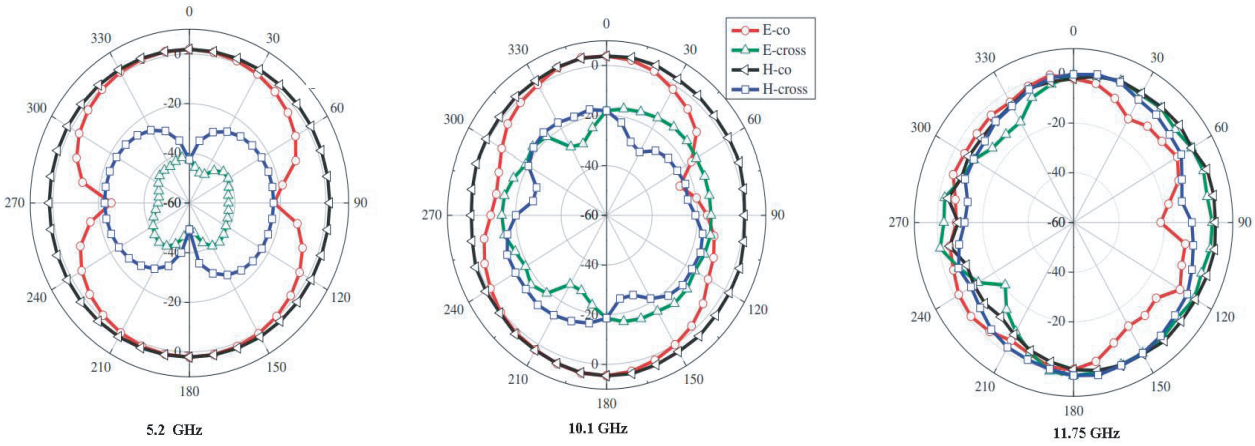

Figure 12. Polarization patterns of the proposed antenna (Simulated).

Table 3. Comparison of reported antennas.

Ref.	Dimensions (mm^3)	Bandwidth (GHz)	Max Peak Gain (dBi)
[2]	$24 \times 28 \times 0.787$	2.76–12.8	5.3
[3]	$25 \times 25 \times 1.6$	2.6–13.04	4.25
[4]	$40 \times 48 \times 1.6$	3.06-12.37	10.07
[5]	$30 \times 27 \times 1.6$	2.7–12	5
[6]	$35 \times 35 \times 1.6$	3.1–12	4.5
[7]	$35 \times 30 \times 1.6$	3.2–12	4.85
[8]	$25 \times 17 \times 1.6$	2.94–22.2	5.18
[9]	$30 \times 31 \times 1.5$	3.1–10.6	—-
[12]	$50.5 \times 48.5 \times 2.08$	3.5&5.8	—-
[13]	40×50	2.1–12.70	3.3
[14]	$40 \times 42 \times 0.75$	2.8–10.9	—-
Proposed	$15 \times 20 \times 1.6$	2.9–14.8	4.9

for UWB applications. A summary of the comparisons is provided in Table 3. Table 3 reveals that the proposed antenna's dimension is the smallest. The suggested novel-designed antenna offers superior gain characteristics to the other reported works while taking up much less space to facilitate UWB communication. Additionally, it has been discovered that the antenna produces better time- and frequency-domain properties. The design and structure methods are also quite innovative.

3.3. Time Domain Analysis

Two identical proposed antenna designs were placed face-to-face (F2F) and side-by-side (S2S) with a 15 cm separation. A Gaussian pulse is sent out by each transceiver, and the other transceiver receives it. Fig. 13 illustrates each configuration's transmitted [(st(t)] and received [(sr(t)] pulse amplitudes. The fidelity factor is 83% in F2F and 71% in S2S.

3.4. Equivalent Circuit Model

In addition, an analogous circuit model for the entire antenna structure might be built by the stages of antenna configuration evolution, as illustrated in Fig. 14. Equivalent model is constructed, tweaked,

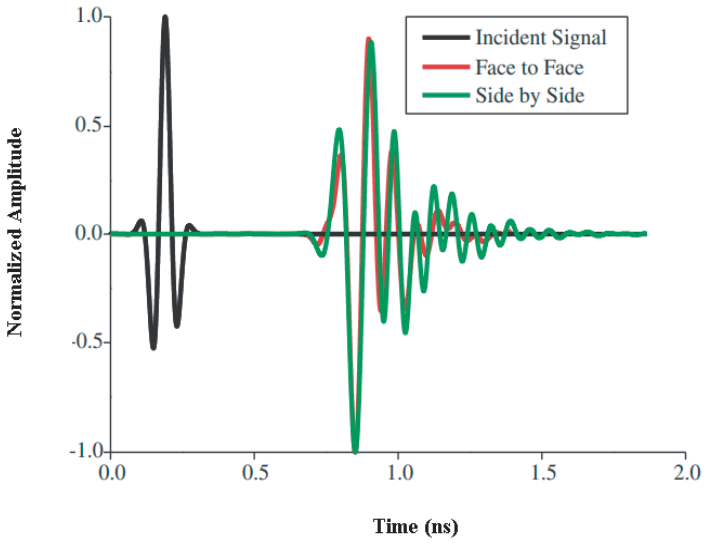

Figure 13. Time domain analysis of the proposed antenna.

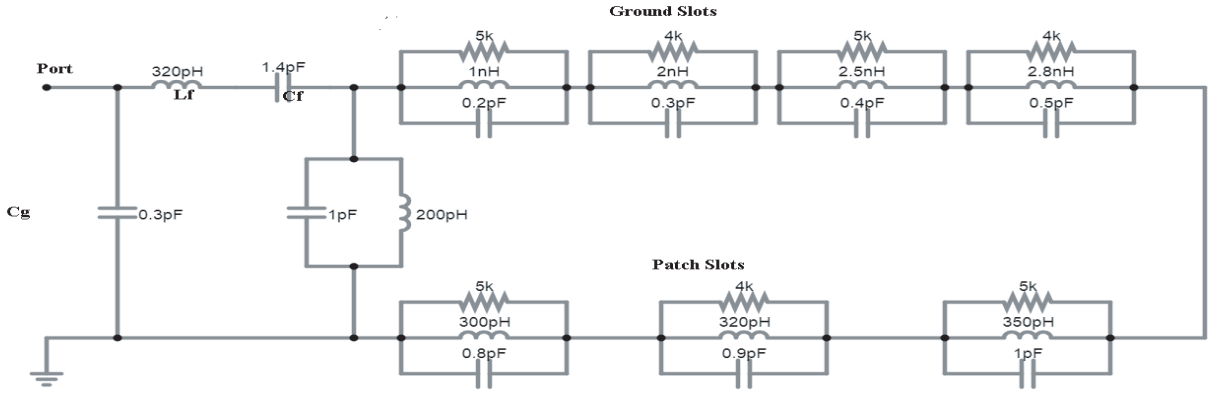

Figure 14. Equivalent circuit model with all parametric values.

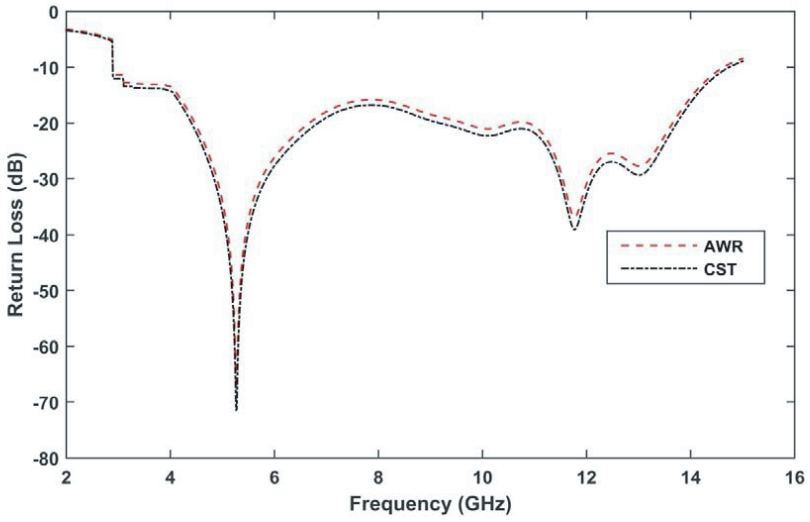

Figure 15. Simulated and equivalent circuit model response.

and optimized by the AWR simulator to validate the antenna structure. Curve-fitting and iterative approaches are used to calculate the values of circuit component values. All calculated numbers are shown in Fig. 14, and observed results of simulated return loss are in Fig. 15.

4. CONCLUSION

A flower-shaped antenna was created utilizing a straightforward fabrication method on a substrate of frequently available daily-wear denim, making it very affordable and durable. Copper cloth is also used to create the patch and ground. For ordinary wearable functions, both fabrics are more comfortable and more flexible than other fabrics. People are inspired to wear by the appealing flower-shaped patch. This compact structure of UWB antenna provides larger impedance bandwidth from 2.9 to 14.8 GHz. The proposed antenna can attain a minimum radiation efficiency of 88.5% across the whole operational band and a maximum peak gain of 4.9 dBi at 5.2 GHz.

This antenna would be beneficial for UWB applications, mobile applications, wireless applications, satellite applications, radio determination applications (4.5–7 GHz and 13.4–14 GHz), etc. due to the advantages of compact size and broader bandwidth compared to other antenna structures. The electrical equivalent circuit of the designed UWB antenna is then given depending on the impact of each slot and antenna element. The designed antenna results produced from the CST simulator software are remarkably similar to the simulated results of the circuit model. Additionally, the performance of the antenna in terms of gain, fractional bandwidth, and antenna size has been compared with previously published similar research works, as shown in the comparison table. In contrast to existing antennas, the suggested antenna is small and has multiband, high gain, and a directed design.

ACKNOWLEDGMENT

My sincere thanks to Dr. T. Shanmuga Nantham for his support throughout this work.

REFERENCES

1. FCC 1st report and order on Ultra-Wideband Technology, Feb. 2002.
2. Koohestani, M. and M. Golpour, "U-shaped microstrip patch antenna with novel parasitic tuning stubs for ultra-wideband applications," *IET Microwaves, Antennas & Propagation*, Vol. 4, No. 7, 938–946, 2010.
3. Gautam, A. K., S. Yadav, and B. K. Kanaujia, "A CPW-fed compact UWB microstrip antenna," *IEEE Antennas and Wireless Propagation Letters*, Vol. 12, 151–154, 2013.
4. Nella, A., A. Bhowmick, and M. Rajagopal, "A novel offset feed flared monopole quasi-Yagi high directional UWB antenna, *International Journal of RF and Microwave Computer-Aided Engineering*, Vol. 31, No. 6, 2021.
5. Jacob, S., V. A. Shameena, S. Mridula, C. K. Anandan, K. Vasudevan, and P. Mohanan, "Planar UWB antenna with modified slotted ground plane, *International Journal of RF and Microwave Computer-Aided Engineering*, Vol. 22, No. 5, 594–602, 2012.
6. Ali, W. A., H. A. Mohamed, A. A. Ibrahim, and M. Z. Hamdalla, "Gain improvement of tunable band-notched UWB antenna using metamaterial lens for high speed wireless communications," *Microsystem Technologies*, Vol. 25, No. 11, 4111–4117, 2019.
7. Choi, S. H., J. K. Park, S. K. Kim, and J. Y. Park, "A new ultra-wideband antenna for UWB applications," *Microwave and Optical Technology Letters*, Vol. 40, No. 5, 399–401, 2004.
8. Tiwari, R. N., P. Singh, and B. K. Kanaujia, "A modified microstrip line fed compact UWB antenna for WiMAX/ISM/WLAN and wireless communications," *AEU — International Journal of Electronics and Communications*, Vol. 104, 58–65, 2019.
9. Rahman, M., et al., "Compact UWB band-notched antenna with integrated bluetooth for personal wireless communication and UWB applications," *Electronics*, Vol. 8, No. 2, 158, 2019.

10. Elajoumi, S., A. Tajmouati, J. Zbitou, A. Errkik, A. M. Sanchez, and M. Latrach, "Bandwidth enhancement of compact microstrip rectangular antennas for UWB applications," *Telkomnika*, Vol. 17, No. 3, 1559–1568, 2019.
11. El Hamdouni, A., A. Tajmouati, J. Zbitou, H. Bennis, A. Errkik, L. El Abdellaoui, and M. Latrach, "A low cost fractal CPW fed antenna for UWB applications with a circular radiating patch," *Telkomnika*, Vol. 18, No. 1, 436–440, 2020.
12. Wang, C., R. Song, S. Jiang, Z. Hu, and D. He, "Low profile and miniaturized dual-band antenna based on graphene assembled film for wearable applications," *International Journal of RF and Microwave Computer-Aided Engineering*, Dec. 2021.
13. Mishra, N. and S. Beg, "A miniaturized microstrip antenna for ultra-wideband applications," *Advanced Electromagnetics*, Vol. 11, No. 2, 54–60, 2022.
14. Parameswari, S. and C. Chitra, "Compact textile UWB antenna with hexagonal for biomedical communication," *J. Ambient Intell. Human Comput.*, 2021.
15. Kumar, O. P., P. Kumar, and T. Ali, "A compact dual-band notched UWB antenna for wireless applications," *Micromachines (Basel)*, Vol. 13, No. 1, 2021.
16. Doddipalli, S. and A. Kothari, "Compact UWB antenna with integrated triple notch bands for WBAN applications," *IEEE Access*, Vol. 7, 183–190, 2018.
17. Devana, V. N., et al., "A novel compact fractal UWB antenna with dual band notched characteristics," *Analog Integrated Circuits and Signal Processing*, Vol. 110, No. 2, 349–360, 2022.
18. Ebadzadeh, S. R., et al., "A compact UWB monopole antenna with rejected WLAN band using split-ring resonator and assessed by analytic hierarchy process method," *Journal of Microwaves, Optoelectronics and Electromagnetic Applications*, Vol. 16, 592–601, 2017.
19. Yao, L., et al., "Miniaturization and electromagnetic reliability of wearable textile antennas," *Electronics*, MPDI, 2021.
20. Lin, X. and Y. Chen, "Ultra-wideband textile antenna for wearable microwave medical imaging applications," *IEEE Transactions on Antennas and Propagation*, Vol. 68, No. 6, 4238–4249, 2020.
21. Ray, K. P., "Design aspects of printed monopole antennas for ultra-wide band applications," *International Journal of Antennas and Propagation*, Vol. 2008, Article ID: 713858, 8 pages, 2008.
22. Kasi, B., L. C. Ping, and C. K. Chakrabarty, "A compact microstrip antenna for ultra-wideband applications," *European Journal of Scientific Research*, Vol. 67, No. 1, 45–51, 2011.
23. Prombutr, N., P. Kirawanich, and P. Akkaraekthalin, "Bandwidth enhancement of UWB microstrip antenna with a modified ground plane," *International Journal of Microwave Science and Technology*, Vol. 2009, Article ID 821515, 7 pages, 2009.
24. Bhavani, S. and T. Shanmuganantham, "Wearable antenna for bio medical applications," *2022 IEEE Delhi Section Conference (DELCON)*, 1–5, 2022.
25. Bhavani, S. and T. Shanmuganantham, "Analysis of different substrate material on wearable antenna for ISM band applications," *Advances in Communication Systems and Networks. Lecture Notes in Electrical Engineering*, Jayakumari, J., Karagiannidis, G., Ma, M., Hossain, S. (eds), Vol. 656, Springer, Singapore, 2020.
26. Bhavani, S. and T. Shanmuganantham, "Analysis of tumor in the breast using UWB textile antenna," *Microwave and Optical Technology Letters*, May 2022.
27. Bhavani, S., "Wearable microstrip circular patch antenna for breast cancer detection," *2021 IEEE International Symposium on Antennas and Propagation and USNC-URSI Radio Science Meeting (APS/URSI)*, 1273–1274, 2021.